Journal of Cleaner Production 207 (2019) 866–874

Contents lists available at ScienceDirect

Journal of Cleaner Production

journal homepage: www.elsevier.com/locate/jclepro

Detailed characterization of particle size fractions of municipal solid waste incineration bottom ash

E. Loginova [a, *], D.S. Volkov [b], P.M.F. van de Wouw [a], M.V.A. Florea [a], H.J.H. Brouwers [a]

[a] Department of the Built Environment, Unit Building Physics and Services, Eindhoven University of Technology, P.O. Box 513, 5600 MB, Eindhoven, the Netherlands

[b] Lomonosov Moscow State University, Chemistry Department — Analytical Centre of Lomonosov Moscow State University, Leninskie Gory, 1-3a, GSP-1, 119991, Moscow, Russia

ARTICLE INFO

Article history:
Received 18 May 2018
Received in revised form
1 October 2018
Accepted 3 October 2018
Available online 5 October 2018

Keywords:
Leaching test
Municipal solid waste incineration bottom ash
Chemical composition
Potentially toxic element
Environmental impact

ABSTRACT

Municipal Solid Waste Incineration Bottom Ash (MSWI BA) is of increasing interest as a secondary construction material worldwide. In most cases, MSWI BA is used in isolated conditions. However, according to the Dutch Green Deal B-076 in 2012, by 2020 all MSWI BA should be used in a non-sealed environment in the Netherlands. However, freshly produced. MSWI BA normally does not match environmental legislation due to high leaching of chlorides, sulfates, and potentially toxic elements. Because different particle size fractions of MSWI BA are of interest for designing optimized concrete recipes, it is beneficial to analyze the whole range of MSWI BA fractions in detail. In this study, 14 size fractions of MSWI BA were analyzed to determine the total elemental composition and leaching capacity, mineralogical composition, and shape variety of fine particles. From the point of view of mineralogical composition, 6 particle size fractions (<180 μm, 180–500 μm, 0.5–1 mm, 1–4 mm, 4–22 mm, > 22 mm) can be distinguished. All together the analyses showed that almost all fractions of the investigated MSWI BA can be used as secondary building materials. However, because the leaching of fine fractions is 5–10 times higher than of coarse fractions, all these fractions must undergo various treatments to allow them to match the environmental legislation. Thus, to decontaminate MSWI BA from potentially toxic elements, a division into three size groups is suggested: fine (<125 μm), medium (125 μm - 1 mm), and coarse fractions (over 1 mm).

1. Introduction

The most common residual materials generated by municipal solid waste incineration (MSWI) plants involve Bottom Ash (BA), boiler ash, fly ash, and air pollution control residues. Among these solid wastes, MSWI BA is predominant (80% w/w) (Wiles, 1995). The size of MSWI BA particles varies widely, from 0.01 to 100 mm. The primary MSWI BA constituents are noncombustible materials (rocks, slag, glass, etc.), unburnt organic matter (threads, films, etc.), and metal scraps (Aubert et al., 2006).

According to regulations in European countries, MSWI BA can be reused in construction materials if the quantities of Potentially Toxic Elements (PTEs) and salts that can leach into ground water are below a certain threshold. The prevalent amounts of these contaminants are concentrated in heat-recovery ash and grate sifting materials with particle sizes below 1 mm, which are not widely processed and thoroughly analyzed to date because of the laborious and expensive treatment needed for these fractions to match legislation requirements (Keulen et al., 2015). Due to a lack of space for landfills and according to the Dutch Green Deal B-076, by 2020 all the residues from incineration plants should be used in a non-sealed environment or landfilled in the Netherlands. All the materials that were previously discarded need to be treated and reused.

The previous research on MSWI BA properties was mainly focused on the mineralogical characterization, and in particular, the composition of phases bearing heavy metals (Wei et al., 2011). In another study, MSWI BA was analyzed by SEM/EDX with an emphasis on the potentialities of the methods for microstructures of mineral phases and nanophases embedded into vitreous structures (Speiser et al., 2001). Using such an approach, XRD, and chemical speciation, the sources of chlorine and heavy metals in MSWI BA as the main factors of potential environmental risks were studied

* Corresponding author.
E-mail address: E.Loginova@tue.nl (E. Loginova).

https://doi.org/10.1016/j.jclepro.2018.10.022
0959-6526/

Nomenclature

EDX	Energy-Dispersive X-Ray Spectroscopy
FTIR	Fourier-Transform Infrared Spectroscopy
IC	Ion Chromatography
ICP-AES	Inductively Coupled Plasma – Atomic Emission Spectroscopy
LL	Legislation Limit
LOD	Limit Of Detection
LOI	Lost On Ignition
LOQ	Limit Of Quantification
L/S	Liquid to Solid
MSWI BA	Municipal Solid Waste Incineration Bottom Ash
PARC	PhAse Recognition and Characterization
PTEs	Potentially Toxic Elements
RSD	Relative Standard Deviation
SEM	Scanning Electron Microscopy
XRD	X-Ray Diffraction

revealing the possible sources of these hazardous components in the ash (Wu et al., 2016). SEM/EDX microstructure analysis followed by the characterization of the leaching behavior of MSWI BA added to concrete and asphalt mixtures revealed metals that can be retained by these construction materials either physically or through chemisorption; the potential hazard was shown for European and Asian MSWI BA (Tasneem et al., 2015). A combination of several methods (element mapping and PARC, SEM/EDX, and leachate analysis) was used to study the composition and contaminants effect of a 0–4 mm MSWI BA fraction on the cement hydration (Schollbach et al., 2016). The composition of calcium- and silicon-containing phases of alkali-activated MSWI BA was characterized using XRD and FTIR spectroscopy; the comparison of cement-like structures in MSWI BA with Portland cement showed similarities and differences of these materials (Zhu et al., 2018). However, the literature providing comprehensive information about the whole MSWI BA fraction range is rather limited. Among the most relevant to this topic are studies devoted to the use of different grain sizes of treated MSWI BA mineral fractions in designing concrete recipes (Sormunen et al., 2017); however, mineralogy and morphology of the treated material is not discussed. Different particle-size fractions of MSWI BA were investigated, but the fractionation was not very detailed (6 fractions) and fines were studied as a single 0–2-mm fraction (del Valle-Zermeño et al., 2017). Previously, it was suggested that MSWI BA fines, while processing, can be divided into two groups: 0–50 μm and 50 μm–2 mm; however, the reasoning was not presented (Xing and Hendriks, 2006). In general, in the literature related to the fractionation of MSWI BA and its properties, the main shortage is in the number of fractions, leaving uninvestigated the properties and behavior patterns within those undivided fractions. Obtaining a full picture about MSWI BA fractions would make it possible to justify its fractional division for further use instead of unifying fractions presumably similar in properties without supporting it with reliable data. This is especially relevant for fine fractions of MSWI BA which might be used in production of small-grain size lightweight artificial aggregates because treated fines can still be used as fillers (Tang et al., 2017) or in the production of blended cement (Li et al., 2012).

Regarding the environmental impact from hazardous components of MSWI BA, it is primarily important to evaluate their leaching capability (van der Sloot et al., 1997); for this reason, almost every legislation is based on leaching. However, to fully understand latent properties of MSWI BA, it might be beneficial to study not only the leaching properties but the total elemental and mineralogical composition as well.

The literature shows that the knowledge gap is laying in the area of a detailed characterization from two viewpoints: a full material 'portfolio' requires a combination of properties (leaching, elemental, and mineralogical) rather than some of them individually; and a large number of MSWI BA size fractions should be analyzed to prove or disprove the necessity to divide them in a certain way for further analysis, treatment, and utilization.

A complete picture of MSWI BA properties might allow the most adequate assessment of not only which treatment methods to use for a particular fraction, but also to understand whether it should be done at all, and how to most efficiently utilize all fractions (sorbents, metal extraction, building materials, etc.). This can make it possible to use MSWI BA more efficiently as a secondary building material. This can help to analyze, process, and reuse more efficiently materials of this type, reducing the landfilled amount and diminishing the proportion of natural materials used in construction. Possessing a wider picture of MSWI BA fractions would help to effectively reduce its environmental impact by removing toxic substances. In this study, the aim is to assess the vital properties for a detailed set (14 narrow size ranges) of MSWI BA fractions, such as leaching capacity, total elemental, mineralogical compositions, and morphology of fine particles, which, to the best of our knowledge, was not implemented previously.

2. Materials and methods

2.1. Equipment

2.1.1. Inductively coupled Plasma-Atomic Emission Spectroscopy (ICP-AES)

ICP–AES was selected as it provides a rapid and highly sensitive multielemental analysis of MSWI BA and fly ash with a high level of precision and accuracy (Alba et al., 1997; Saqib and Bäckström, 2016). An axial ICP Atomic Emission Spectroscopy (AES) 720-ES spectrometer with an SPS3 autosampler and ICP Expert software 2.0.5 (Agilent Technologies) with a low flow axial quartz torch with a 2.4 mm i.d. injector tube (Glass Expansion), a double-pass glass cyclonic spray chamber, a glass pneumatic nebulizer (Agilent Technologies), and a Trident Internal Standard Kit (Glass Expansion) was used. All emission lines were measured simultaneously. An internal standard solution was added online.

2.1.2. X-ray diffraction (XRD)

The MSWI BA mineralogical composition was determined by XRD using a Bruker D2 PHASER (a Co tube, 1.79026 [Å]) with a LYNXEYE 1-D detector and fixed divergence slits. XRD measurements were performed on pre-dried powdered samples. Phase identification was performed using X'Pert HighScore Plus 2.2 and the PDF-2 database.

2.1.3. Ion chromatography

IC was used as a standard method for chloride and sulfate determination in leachates (Ito et al., 2008). A Thermo Scientific Dionex 1100 ion chromatograph was used: 2 × 250 mm AS9-HS ion-exchange columns, isocratic flow (0.25 mL/min). Ion detection was carried out by measuring a suppressed conductivity with an electrolytically regenerated suppressor (Thermo Scientific Dionex AERS 500 2 mm). A solution of Na_2CO_3 (9 mM) was used as eluent.

2.1.4. Scanning electron microscopy (SEM)

SEM (Phenom ProX, PhenomWorld) with a backscattering electron detector with a spot size of 4.0 and a voltage of 15.0 kV was used. The samples were covered with a 14-nm gold layer by a SOP K575× Dual Turbo sputter coater prior to analysis.

2.1.5. Auxiliary equipment

A lab-scale jaw crusher (Retsch BB 100) fitted with waved manganese steel jaws set to an opening of 8 mm, a planetary ball mill (Fritsch PULVERISETTE 5) fitted with zirconium oxide grinding bowls, and 20 and 10-mm mill balls were employed successfully for the sample size reduction. A chamber furnace (Thermo Scientific Heraeus K 114) was used for Loss On Ignition (LOI) (550 °C). A fusion instrument (Claisse leNEO) was used. Riffle boxes (sample splitters), 15-D0438 and 15-D0438/F (Controls Group), were used to obtain randomly divided samples. An SM-30 shaking table (Edmund Bühler GmbH) was used to perform the leaching test. Automatic Eppendorf Research pipettes (Eppendorf International) were used for the preparation of calibration solutions. A-class polypropylene volumetric flasks (Vitlab) with volumes (50.00 ± 0.12) mL and (100.00 ± 0.20) mL and polypropylene test tubes (Axygen) were used for the preparation of calibration and test solutions. An analytical balance (Mettler Toledo XP 504), a balance (Mettler Toledo ID5 Multirange), and a UF 260 drying oven (Memmert) were used for sample preparation.

2.1.6. Data treatment

The measurement results are presented in accordance with the requirements of ISO/IEC 17025:2005. Limits Of Detection (LODs) and Limits Of Quantification (LOQs) were calculated as the ratios of three and ten times standard deviation of twenty blank readings to the calibration-curve slopes. Concentration detection limits by ICP–AES were recalculated to MSWI BA quantities.

2.2. Samples and reagents

MSWI BA was supplied by the municipal solid waste-to-energy incinerator plant of AVR-Van Gansewinkel (Duiven, the Netherlands). The material had been stored for 3 months after the production, prior to analyses. Deionized water (specific resistance, 18.2 MΩ × cm) from a Milli-Q Academic system (Millipore) and HNO_3 (69%, ACS-ISO grade, Panreac) were used for the preparation of calibration solutions and washing.

A mixture of standard solutions ICP-AM-6 (100 mg/L of Al, Sb, B, Ba, Be, Cd, Ca, Co, Cr, Cu, Fe, Li, Mg, Mn, Mo, Ni, K, Na, Si, Pb, Tl, Sr, V, Zn) and ICP-MS-68B (100 mg/L of Sb, Ge, Hf, Mo, Nb, Si, Ag, Ta, Te, Sn, Ti, W, Zr) from High-Purity Standards was used for the calibration in the range 0.01–10 mg/L. A mixture of an ICP-AM-15 standard solution (10000 mg/L of Na, K, Ca, Mg), P (10000 mg/L) and S (10000 mg/L) was used for the calibration in the range 1–100 mg/L. An internal-standard solution of Sc (20 mg/L) was prepared from a standard solution (Inorganic Ventures, 1000 mg/L).

2.3. Procedures

2.3.1. Sample preparation

Due to high heterogeneity of MSWI BA, three samples (the fraction above 12 mm, 15 kg each) were used as replicate samples. Prior to analysis, samples were crushed to break agglomerated or cemented materials, then ferrous and nonferrous metals were extracted. Further, the material was dried in an oven at 105 °C to a constant mass. Next, to obtain the entire range of fractions, each sample was sieved into 19 size fractions according to EN 933-1 (2012) and EN 933-2 (1995) with the addition of sieves with the following mesh sizes: 22.4 mm, 11.2 mm, 5.6 mm, 2.8 mm, 1.4 mm, 710 μm, 355 μm, 180 μm, and 90 μm to provide more fractionation of coarse fractions and to render the initial detailed set of similarly distributed fractions for coarse, medium, and fine fractions. Then, some of these sieved fractions were unified if they had insufficient mass to be analyzed. This resulted in the set of 14 fractions: < 63 μm, 63–90 μm, 90–125 μm, 125–180 μm, 180–250 μm, 250–355 μm, 355–710 μm and 0.71–1 mm, 1–2 mm, 2–2.8 mm, 2.8–4 mm, 4–11.2 mm, 11.2–22.4 mm, and >22.4 mm. Each fraction of replicates was divided with sample splitters: the first half was saved for later use for total quantitative analysis by ICP–AES; the second half was used for a leaching test. Next, the particle size was reduced using a crusher and a planetary ball mill to prepare samples for borate fusion (required particle size less than 500 μm). Fractions with a particle size >4 mm were both crushed and milled. Fractions with a particle size from 500 μm to 4 mm were milled without crushing. Each fraction was milled at 200 rpm for 1 h and 40 min with a 5 min break every 10 min. After milling, fractions larger than 500 μm were sieved through a 500-μm sieve to remove unmilled matter (generally, flattened metal particles, threads, rope pieces, etc.). The largest content of these components in the studied fractions was in the range of 1% w/w.

2.3.2. Leaching test

Every fraction sample (Section 2.3.1) was subjected to the leaching test according to EN 12457-4. Upon completion (24 h of shaking, L/S 10), all the leachates were filtered (0.2 μm) to prepare them for later analyses by IC (Section 2.1.3) and ICP–AES (Section 2.1.1).

2.3.3. Fused bead preparation

To prepare fused beads, the following procedure was used: 0.95 g of MSWI BA was mixed with 9.5 g of a flux (67.00% $Li_2B_4O_7$ – 33.00% $LiBO_2$, Claisse) and 0.1 g of LiBr (Claisse) as a non-wetting agent. Mixtures were put individually into borate fusion ovens for 24 min at 1065 °C. The procedure was made for 3 replicates for all the fractions.

The borate-fusion technique allows rapid and easy sample preparation to conduct a subsequent mutielemental analysis using ICP–AES. Compared to microwave digestion, which frequently causes difficulties with a factually complete sample dissolution (Kolev and McKelvie, 2008; Matusiewicz, 2017), a sample is completely dissolved. A blend of lithium metaborate and tetraborate was selected as a mixture of basic and acidic fluxes, which provide a complete and reproducible sample preparation of industrial waste BA including different incinerator types (Iwata et al., 2004), various types of slag (blast furnace, steel) (Fällman and Hartlén, 1994), and MSWI BA (Abbas et al., 2003) as all these residues contain both types of oxides.

2.3.4. Elemental determination

Fused beads were ground for 2 min in a planetary ball mill, and 1-g weighed portions were dissolved in 50.00 mL of 5% HNO_3 (p.a. grade) in an ultrasonic bath for 1 h and subjected to ICP–AES. The estimated average concentrations of designated elements (μg/mL) were recalculated to mg per 1 kg of the raw material.

3. Results and discussion

3.1. SEM of fine MSWI BA fractions

A SEM analysis was conducted to discover differences in the shape and structure of MSWI BA particles among the fine fractions up to 500 μm. Among the literature on the topic, no SEM research on different particle size fractions of this material was made previously. Among the newest studies, the outlook (Gao et al., 2017) and photos of MSWI BA particles ground below 45 μm (Wongsa et al., 2017) can be found. Fig. 1a illustrates the shape of particles from the finest fraction. Particles of this fraction, which have a very small size (about 20 μm) and a large surface, are predominant. There are only a few large particles, and their surface appears to be similar to the one of the smallest MSWI BA particles. For the

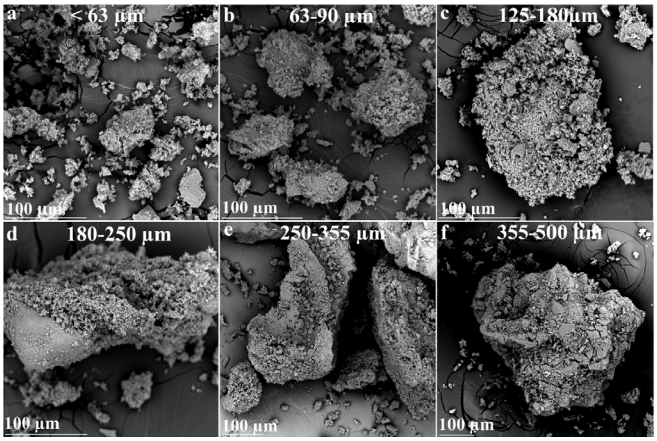

Fig. 1. SEM images of MSWI BA fine particle size fractions.

fraction 63–90 μm (Fig. 1b), despite the obvious predominance of fairly large particles with developed surfaces, tiny particles about the same size of 10–20 μm and even smaller are also present, Fig. 1a.

Fig. 1 c and d illustrate the appearance of 125–180 and 180–250 μm fractions at the same scale as the previous ones. They have the same highly developed surface, and there are also very small particles nearby, but much less. Fig. 1e and f shows the remaining fractions from the fine-size range with a larger scale. The shape of the particle surface does not differ from 125 to 250 μm. Particles of at least 500 μm are significantly different from those of larger fractions (which resemble very small pieces of rock, glass, etc.), and the morphology does not differ among fine fractions. These particles, called quench products, are formed during water spraying on hot MSWI BA after the incineration (Chimenos et al., 1999). They have amorphous and microcrystalline structures mainly consisting of calcium silicate hydrate with the particle size below 0.4 mm (Inkaew et al., 2015). These quench products adhere to larger particles, forming a fragile surface layer. It was shown that the quenching phase of MSWI BA processing highly affects the leaching of PTEs (Marchese and Genon, 2011). Their developed surface of these particles, serving as a high-capacity absorbent, might be a source of their significant release during their subsequent use in building materials (Dabo et al., 2009; Liu et al., 2008).

3.2. Mineralogical composition of MSWI BA fractions

The 14 original MSWI BA fractions, mineralogically, can be divided into six combined groups, Table 1. The minor fractions are virtually the same in composition, so in Table 1 and on Fig. 2 groups of fractions are presented to avoid the duplication of information.

Quartz is prevalent in all the fractions. This is in line with literature as the main mineral in fine fractions below 2 mm (Minane et al., 2017) and coarse fractions, 2–50 mm (Lin et al., 2015). Due to a mechanical resistance, the amount of quartz in the fractions increases with the particle size (Fig. 2). Two other components, which are also present in all fractions but in slightly different amounts, are feldspar and magnesium ferrite, which were also found previously (Saffarzadeh et al., 2011).

The next group of minerals — melilite, spinel, and pyroxene — are present in all fractions except <180 μm (Dabo et al., 2008). Sylvite, as well as its modifications (all denoted as S) containing different amounts of K and Na, is present in all fractions except the largest one (>22 mm), which agrees with the leaching test results for these fractions (Section 3.4.1). In fractions below 4 mm and in

Table 1
Main mineral phases in the composition of 6 combined particle size fractions of MSWI BA.

Mineral	<180	180–500	0.5–1	1–4	4–22	>22
	μm		mm			
Quartz	+	+	+	+	+	+
Feldspar	+	+	+	+	+	+
$MgFe_2O_4$	+	+	+	+	+	+
Melilite	–	+	+	+	+	+
Spinel	–	+	+	+	+	+
Pyroxene	–	+	+	+	+	+
Sylvite	+	+	+	+	+	–
Zeolite	+	+	+	+	–	+
Calcite	+	+	+	+	–	–
Anhydrite	+	+	–	–	–	–
Halite	+	–	–	–	–	–
Mica	–	–	–	–	–	+

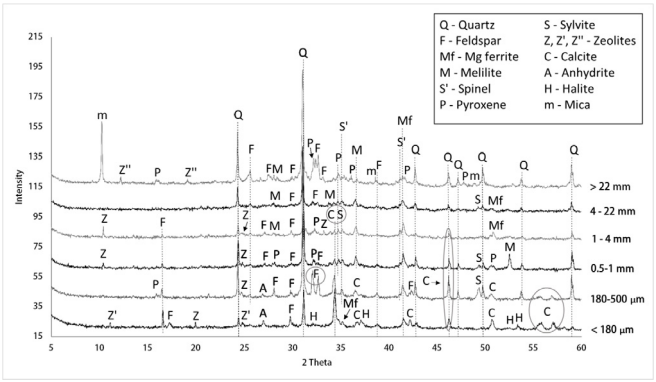

Fig. 2. Diffractograms (a Co tube) of 6 combined MSWI BA fractions; for the sake of convenience, the plots are shifted relative to each other; the intensity scale is given in square roots of original values.

the largest fraction, traces of zeolites of various composition were found. Their absence in 4–22 mm fractions can be explained by the fact that zeolites have a domestic source represented by sufficiently fine particles, e.g. washing powders (Hui and Chao, 2006), adsorbents (Vasiliev et al., 1996), which, in the incineration process, are more likely to end up in MSWI BA fine fractions. The presence of zeolites in the largest fraction can be explained by attached fine particles (Chimenos et al., 1999). Calcite and anhydrite are commonly found in MSWI BA phases (Saffarzadeh et al., 2011). Calcite can be seen in all fractions below 4 mm. Anhydrite is present in fractions below 500 μm, which agrees with the leaching test results for sulfate, a steep decline in sulfate leaching after the 500 μm fraction (Fig. 6).

Halite is detected in fractions below 180 μm only. The last mineral that distinguishes the largest fraction from all the others is mica. This could be explained by the fact that micas are widely used in the glass manufacture, from decorative to optical (Grossman, 1972), and the glass share in the largest fraction is (visually) larger compared to fractions below 22 mm.

The predominant phases in the investigated MSWI BA are quartz and various aluminosilicates, which makes it possible to consider all the fractions as secondary building materials. The results agree with the literature (Wei et al., 2011).

3.3. Total elemental composition of MSWI BA fractions

The major elements found in MSWI BA fractions were Si, Ca, Fe, Na, S, and Mg, which is in accordance with mineralogical data

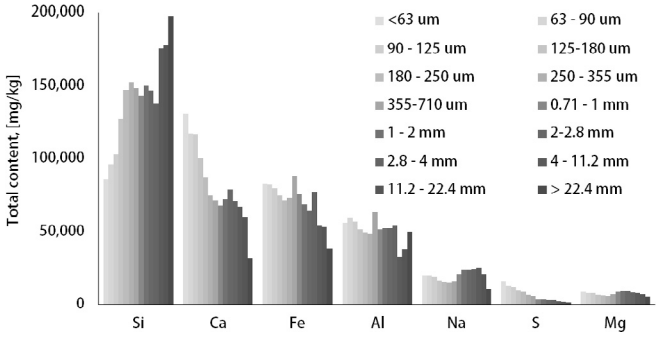

Fig. 3. Total content of major elements in 14 particle size fractions of MSWI BA.

(Section 3.2) and literature (Zevenbergen et al., 1994). Fig. 3 demonstrates that concentrations of Ca, Fe, and S decrease as the particle size increases. The trend for Si is the opposite. The contents of Na, Al, and Mg vary insignificantly among fractions, but there is no decreasing trend.

Fig. 4 illustrates the particle-size dependence of the content for elements present in medium concentrations in the MSWI BA, including PTEs; there is not a full set of data for these fractions and elements in the literature. In all cases, there is a gradual decrease in the concentrations of all the elements for fines below 355 μm. This agrees with SEM data on the same particle shape for these fractions and is caused by the specific surface area of these particles and quench-product particles. A significant increase in concentrations for larger-size fractions is observed, which is due to a change in the mineralogical composition of particles; this effect is strongest for Cu (1–2.8 mm) and Zn (2–4 mm). To the best of our knowledge, this is observed for the first time. The Ti content varies insignificantly among fractions above 355 μm (3200–4000 mg/kg). Similarly, Ba and Mn contents remain approximately at the same level with insignificant fluctuations among fractions above 355 μm. The contents of Cr, Pb, Ni, and Sb decrease smoothly and with fluctuations with an increase in the particle size.

Table 2 presents the Relative Standard Deviation (RSD) values for all investigated particle size fractions of MSWI BA for all the elements in this study. The results for 3 replicates show negligible differences for most elements and fractions. Higher RSDs for Cd, Sb, and Sn for some fractions might be explained by the trace level of concentrations (Cd max. 14 mg/kg, Sb max. 170 mg/kg, and Sn max. 350 mg/kg) for these elements. As during the preparation, samples were significantly diluted, this might be considered as one of the limitations of this method to investigate trace elements.

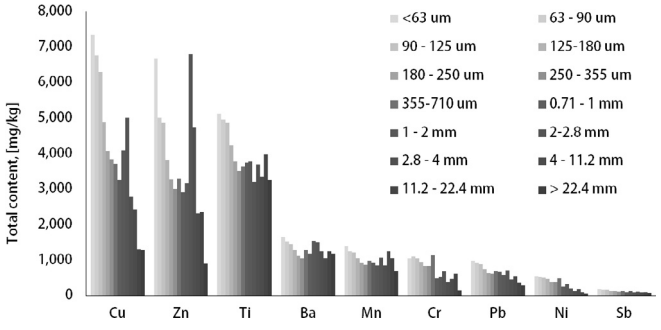

Fig. 4. Total content of PTEs and medium concentrated elements in 14 particle size fractions of MSWI BA.

Table 2
RSD values for total microelemental determination for 14 particle size fractions of MSWI BA ($n = 3$).

P.size|Element	Al	Ba	Ca	Cd	Co	Cr	Cu	Fe	Mg	Mn	Na	Ni	Pb	Si	Sr	Sb	Sn	Ti	V	Zn	S	P
<63 um	0.13	0.096	0.024	0.22	0.110	0.11	0.071	0.010	0.072	0.015	0.049	0.15	0.066	0.068	0.062	0.12	0.010	0.10	0.12	0.018	0.032	0.089
63 - 90 um	0.12	0.15	0.045	0.041	0.015	0.13	0.073	0.018	0.088	0.038	0.030	0.088	0.019	0.057	0.091	0.19	0.042	0.10	0.14	0.043	0.022	0.10
90 - 125 um	0.10	0.11	0.081	0.17	0.075	0.15	0.061	0.019	0.11	0.045	0.026	0.057	0.047	0.018	0.14	0.19	0.057	0.10	0.11	0.11	0.18	0.086
125-180 um	0.13	0.079	0.029	0.081	0.012	0.16	0.083	0.016	0.076	0.038	0.033	0.066	0.014	0.075	0.077	0.15	0.054	0.092	0.10	0.042	0.011	0.083
180 - 250 um	0.13	0.10	0.060	0.19	0.074	0.15	0.068	0.015	0.079	0.025	0.041	0.048	0.029	0.037	0.076	0.19	0.11	0.10	0.11	0.043	0.100	0.12
250 - 355 um	0.11	0.12	0.028	0.12	0.030	0.092	0.052	0.056	0.057	0.023	0.071	0.16	0.014	0.070	0.073	0.25	0.20	0.10	0.12	0.025	0.050	0.088
355-710 um	0.14	0.22	0.013	0.013	0.19	0.15	0.051	0.047	0.060	0.071	0.066	0.16	0.028	0.092	0.037	0.17	0.028	0.081	0.12	0.10	0.27	0.093
0.71–1 mm	0.16	0.10	0.053	0.015	0.028	0.084	0.060	0.049	0.085	0.12	0.071	0.11	0.074	0.041	0.074	0.19	0.019	0.12	0.14	0.012	0.082	0.040
1–2 mm	0.061	0.048	0.017	0.29	0.11	0.071	0.13	0.039	0.047	0.053	0.045	0.098	0.054	0.027	0.064	0.018	0.39	0.064	0.030	0.049	0.13	0.044
2–2.8 mm	0.046	0.060	0.041	0.017	0.15	0.054	0.029	0.035	0.013	0.026	0.084	0.031	0.012	0.015	0.077	0.039	0.022	0.011	0.038	0.098	0.023	0.020
2.8–4 mm	0.085	0.091	0.011	0.016	0.070	0.20	0.076	0.026	0.019	0.066	0.041	0.017	0.55	0.013	0.053	0.17	0.088	0.019	0.12	0.027	0.022	0.020
4–11.2 mm	0.045	0.007	0.040	0.011	0.051	0.032	0.033	0.031	0.014	0.037	0.047	0.055	0.037	0.028	0.042	0.094	0.49	0.011	0.021	0.097	0.052	0.34
11.2–22.4 mm	0.049	0.069	0.016	0.013	0.11	0.075	0.18	0.041	0.028	0.097	0.012	0.11	0.017	0.014	0.043	0.046	0.18	0.093	0.017	0.058	0.088	0.056
>22.4 mm	0.034	0.13	0.059	0.019	0.028	0.26	0.22	0.18	0.012	0.26	0.13	0.037	0.15	0.018	0.068	0.21	0.15	0.10	0.014	0.081	0.013	0.13

3.4. Leaching test and its fraction dependences

For total analysis, the elements forming major basic (Na, Mg, Ca, Ba) and acidic (Si, P, S) oxides in MSWI BA, and medium-concentration (Al, Cu, Zn, Ti, Cr, Mn, Fe, Co, Ni) and trace (V, Sr, Zr, Sn, Sb, Pb) elements (Liu et al., 2008) were selected; out of these, only a few exceed the environmental Legislation Limits (LL) in MSWI BA, which are shown in Table 3.

3.4.1. Major cations and anions

Table 4 shows the pH over the range of fractions. It varies between 8.8 and 9.2 and does not account for differences between the leaching behavior of the samples.

The shapes of the concentration dependences in MSWI BA fraction leachates on the particle size of the corresponding fraction for the main cations (Ca, Na, and K) are quite similar to each other (Fig. 5). For fines, a rather steep decrease after 125 μm is observed for all cations, and after 0.71–1 mm fraction, the concentration level does not change significantly, generally decreases and reaches a plateau. The shapes of these curves are very similar as well to the curve shapes for sulfate and chloride (Fig. 6). This might be an indication of a similar mechanism of dissolution of components which consist of major cations and anions. Such data can be attributed to the overall increase in the particle specific surface area with the decrease in its size together with changes in the matrix and the particle shape. It is changing from round packed (stones, pieces of glass, etc.) to less dense particles (Fig. 1) with a substantially higher specific surface area and agrees with the literature (Dahl et al., 2009).

Major cations and chloride and sulfate may affect the leaching behavior of medium-concentration and minor cations (Polettini et al., 2009). The leached amounts of sulfate and chloride among fractions show a similar pattern (Fig. 6).

Table 3
Maximum allowable leaching (LL) for non-shaped building materials according to The Soil Quality Decree.

Element	Cd	Cr	Cu	Ni	Sb	Zn
LL (mg/kg)	0.04	0.63	0.9	0.44	0.32	4.5

Table 4
pH of 14 particle size fractions of MSWI BA.

No.	μm	pH	No.	mm	pH
1	<63	8.9	8	0.71–1	8.9
2	63–90	8.9	9	1–2	9.1
3	90–125	8.8	10	2–2.8	9.0
4	125–180	8.8	11	2.8–4	9.2
5	180–250	8.8	12	4–11.2	9.1
6	250–355	8.8	13	11.2–22.4	9.1
7	355–710	8.9	14	>22.4	9.2

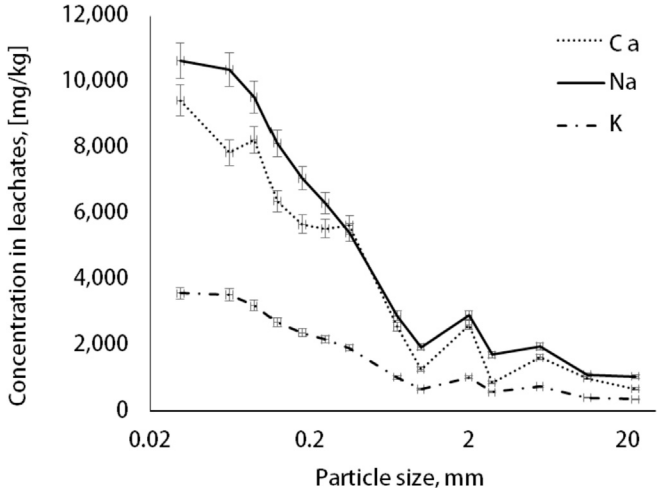

Fig. 5. Leaching of major cations (Ca, Na, and K) related to the MSWI BA particle size. X-axis values are shown on a logarithmic scale.

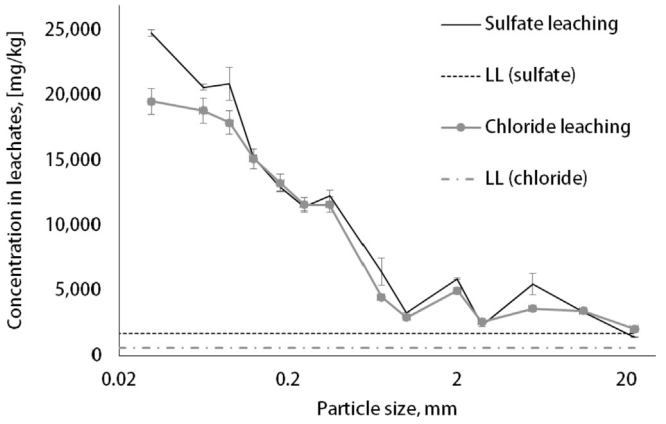

Fig. 6. Chloride and sulfate leaching related to the MSWI BA particle size. X-axis values are shown on a logarithmic scale.

3.4.2. PTEs

The leachability dependence on particle size is shown in Fig. 7 for PTEs which are present in the studied MSWI BA and if their level is higher than the LL (Ni, Cu, Zn, and Sb). For Co, Cr, Mo, Pb, Sn, Cd, and V concentrations in leachates are below LOQs (<0.05 mg/kg recalculated to the sample mass).

3.4.2.1. Copper. A high level of copper leaching is a common challenge in MSWI BA processing (Yao et al., 2010) due to the ability of Cu to transform into stable inorganic compounds, e.g. $Cu(OH)_2^0$, $Cu_4(OH)_6SO_4 \cdot 1.3H_2O$ (Meima and Comans, 1999) and to form stable and readily soluble complexes with organic ligands (Sunda and Lewis, 1978). These copper compounds are readily distributed in many materials and living organisms (Lam et al., 2010). Concentrations above the LL were found for all fractions of 500 μm and lower and for some coarse ones (Fig. 8a).

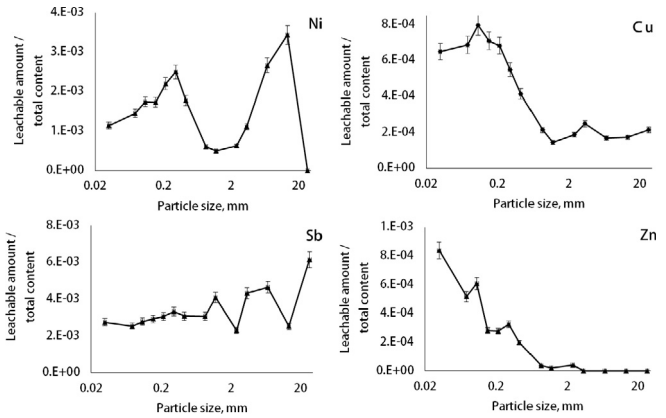

Fig. 7. Leaching capacity (percentage of the total) *vs.* fraction size for Ni, Cu, Zn, and Sb. X-axis values are shown on a logarithmic scale.

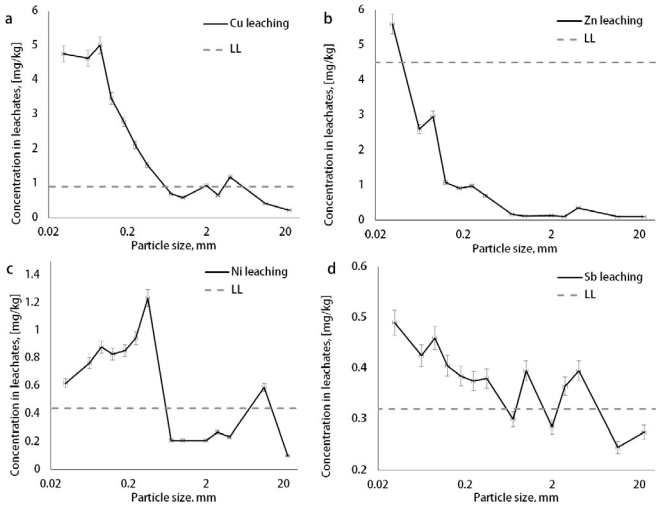

Fig. 8. Leaching of Cu (a), Zn (b), Ni (c), Sb (d) related to the MSWI BA particle size. X-axis values are shown on a logarithmic scale.

As exceeding the limit of leachable copper content in these fractions is not too high (32 and 77 percent above the limit) in comparison with finer fractions (up to 6-fold higher than the limit); it can be concluded that its source is also the attached fine-particle layer (Section 3.1). The difference between the leaching levels of different metals in the coarse fractions attributed to this reason might be explained by the difference in content/leaching of corresponding metals in fines. If the metal leaching in the finest fraction exceeds the LL by several times it might be enough to contaminate the whole fraction. If the leaching of a certain metal in the most contaminated fraction merely exceeds that limit, then due to a low share of fines in a coarse fraction, the overall leaching of this coarse fraction can be still low. Though the amount of copper in the leachates of fines exceeds the LL, the leaching capacity of copper is not very high (Fig. 7). Among fine factions, it decreases from 0.08% to 0.01% w/w and then remains at this level.

3.4.2.2. Zinc. Despite the relatively significant zinc content in the MSWI BA (Fig. 7), exceeding the LL is only observed in the finest fractions (Fig. 8b). Together with a linear decrease in Zn total content down to 710 μm (Fig. 9), the zinc concentration in leachates decreases in the same manner as Cu. Then it reaches a plateau, even though Zn total content varies significantly (Fig. 9).

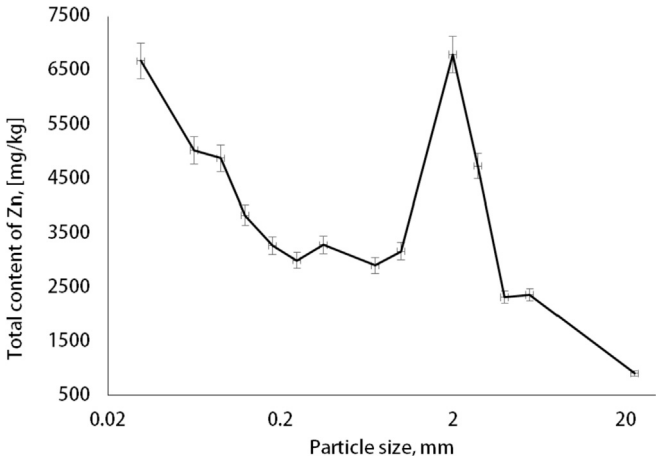

Fig. 9. Zn total content related to the MSWI BA particle size. X-axis values are shown on a logarithmic scale.

3.4.2.3. Nickel. Leaching concentrations above the limit were found in all fine fractions 500 μm and lower (Fig. 8c). Also, the leachate concentration was slightly above the limit in the 4–11.2-mm fraction, which, as in almost all cases in this study, is most likely due to attached fine particles (Section 3.1).

The Ni leaching capacity is still quite low compared with the prevailing ions (chloride, Na, Mg, and K); in the most contaminated fractions only 0.35% w/w of Ni total content transfers into a leachate (Fig. 7). In fractions with no LL exceeding, less than 0.13% w/w of total Ni migrates into the leachate. Unlike most other elements, the leaching capacity of Ni has no distinct trend among fines, with the leached amount dropping but then increasing steeply with a peak for 4–11.2-mm fraction (Fig. 7). A correlation between the total content of Ni in the MSWI BA and its leaching capacity is not observed.

3.4.2.4. Antimony. The Sb leaching from MSWI BA is a well-known problem (Dijkstra et al., 2006); the literature on antimony leaching is mainly focused on the influence of pH, carbonation, and weathering of MSWI BA (Cornelis et al., 2012) or mineral additives and organic acids (Verbinnen et al., 2017), but not on leaching dependence on particle size. Sb values exceeding or very close (for two fractions 0.30 and 0.29 mg/kg) to the LL (Table 3) are found in all fractions below 4 mm (Fig. 8d). In contrast to other PTEs, the antimony content in the leachates of fines does not vary significantly (Fig. 7), and its leaching capacity is in the range of 0.2–0.5% w/w, regardless of the particle size.

The leaching of other elements that might pose an environmental risk (Table 5) might have not been observed for two main reasons: firstly, they are present in MSWI BA samples in low or trace amounts; secondly, these elements leach very low (see Table 4) or not at all at such pH conditions (Quina et al., 2009).

The leaching test and total analysis show that a linear correlation between the total amount of an element and its leaching capacity is not observed for any of the test elements. However, some leaching curves (major cations, anions, Cu, and Zn) have similar shapes with higher leaching in the region of fines (up to 125 μm) with a steep decrease for fractions above 0.5 mm and a plateau for coarse fractions 1 mm and larger (Figs. 5 and 6, and Fig. 8a, b).

3.5. Division of MSWI BA for decontaminating treatments

Based on the leaching data, total elemental composition, and mineralogical analysis, the studied MSWI BA is suitable for use in building materials, with the condition that a pretreatment adequate to the level of contaminants is performed. Because MSWI BA fines (<125 μm) are the most contaminated and leach significantly more than coarser fractions and show morphology and mineralogy different from larger fractions, it is advised to separate them from the rest of the material for the following washing treatment, to not contaminate the fraction above 125 μm. Mineralogically, morphologically, and even total element content-wise all three fractions below 125 μm are virtually the same.

Table 5
Total content of PTEs present in MSWI BA samples (the range over 14 particle-size fractions, 0–22.4 mm).

Element	Total content (mg/kg)
Cd	0–14
Co	100–250
Cr	100–1400
Pb	200–1000
Sn	50–350
V	0–40

Table 6
Ranges of concentrations of PTEs and anions in 3 combined (for further treatment) fractions of MSWI BA.

Component	<125 μm	125 μm–1 mm	over 1 mm
	mg/kg		
Total PTE leaching (Cu, Ni, Sb, Zn)	8–12	4.5–6.5	0.65–2.5
Chloride	18,000–20,000	12,000–15,000	2000–4500
Sulfate	20,000–25,000	6000–15,000	1500–3500

Fractions from 125 μm to 1 mm are far less contaminated and yet demanding a treatment against both anions (Cl^- and SO_4^{2-}) and cations (see Section 3.4.2). Mineralogically, they do not differ significantly as well, so they can be combined in a single medium fraction from the viewpoint of treatment and use.

The coarsest fraction (>1 mm) is just slightly contaminated with anions and mostly free from large amounts of leachable PTEs; this part of the material needs just a slight washing with water, after which it can be divided for further applications based on the total content of elements and mineralogical composition.

Hereby, for purifying MSWI BA from PTEs, Cl^-, and SO_4^{2-} a size division into three groups is suggested: fine (<125 μm), medium (125 μm–1 mm), and coarse fractions (over 1 mm). Table 6 shows the ranges of concentrations of PTEs and anions in combined groups of fractions, which have different concentration levels of all these components.

As for coarse fractions, a slight water treatment would be sufficient, while the medium and fine fractions require a more intense treatment, because PTEs and anion concentrations exceed the limits by several times. It should be noted that during the water treatment of a coarse fraction, the process of elimination of attached fines, which are the main source of the coarse fraction contamination, is vital. In comparison with previous research (Xing and Hendriks, 2006), a more distinct criterion related to fractional division of MSWI BA is obtained. This should help in increasing the MSWI BA purification process efficiency, as well as creating more economically feasible treatments.

4. Conclusions

Based on the leaching data, total elemental composition, and mineralogical analysis, dividing MSWI BA into groups is suggested for different purposes according to their properties. Hereby, it is suggested to consider various properties of a fraction potentially applied for a certain application (building materials, adsorbents, metal extractions, etc.), to justify the suitability of the selected way of reuse/recycling.

From the point of view of the mineralogical composition, 6 particle size fractions (<180 μm, 180–500 μm, 0.5–1 mm, 1–4 mm, 4–22 mm, > 22 mm) can be distinguished, because the smaller fractions that form groups with similar compositions. The morphology in small-size fractions (up to 500 μm) also does not differ. It is worth mentioning that the leaching shows that the developed surface of these particles provides not only efficient absorption of PTEs, water, etc, but also their release in case of their further use. The total analysis of MSWI BA fractions confirms a possibility for using it in building materials after a suitable pre-treatment. It is vital to consider the limitations such as chemical properties, mineral composition, and the particle structure features. The main insight that can be derived is that it would be beneficial, and, perhaps, easier in some cases to eliminate sources of PTEs in waste rather than deal with these contaminants afterwards.

To decontaminate MSWI BA from PTEs, the final size division into three groups is suggested: fine (<125 μm), medium (125 μm–1 mm), and coarse fractions (over 1 mm). This is most beneficial from the economical point of view because the treatments that these three fractions should undergo would vary significantly in cost. In the case of washing coarsest fractions, with the help of the division process they will not be contaminated with fines which are responsible for a fair share of the leaching. Such information on the MSWI BA properties, including the leaching dependences *vs.* the total element composition, mineralogical composition, and morphology of fines, will allow faster and more efficient analysis of waste materials such as MSWI BA. Based on these data, appropriate treatments can be applied to successfully use them in building materials.

This study was carried out only on one MSWI BA material (one country, one plant), and we consider the result as a primary empirical generalization. It seems possible to develop empirical models of PTE leaching to predict the expected range of concentrations in leachates of different MSWI BA fractions without conducting the leaching analysis. To reach this goal, it seems necessary to obtain similar MSWI BA datasets for different plants, countries, and seasons. On top of that, it would be expedient to study the behavior of different fractions and the fractionation effect on the properties of building materials in which MSWI BA can be used. Further studies should also include the development of a MSWI BA treatment procedures which are appropriate for the contamination level and MSWI BA chemical properties, which would ensure matching the environmental legislation.

Acknowledgements

The authors express their gratitude to the NWO/TTW-foundation (project 13318, Development of eco-concretes by using industrial by-products), Van Gansewinkel Minerals, Attero, ENCI, v.d. Bosch Beton, StruykVerwo, and CRH Europe Sustainable Concrete Centre for their provision of material, knowledge and financial support in this project, as well as to the Cement-Concrete-Immobilisates sponsor group at TU Eindhoven: Rijkswaterstaat Grote ProjectenenOnderhoud, Graniet-Import Benelux, KijlstraBetonmortel, Rijkswaterstaat Zee en Delta - District Noord, BTE, Selor, GMB, Geochem Research, Icopal, BN International, Eltomation, KnaufGips, Hess AAC Systems, Kronos, Joma, Cement&BetonCentrum, Heros, Inashco (chronological order of joining).

References

Abbas, Z., Moghaddam, A.P., Steenari, B.-M., 2003. Release of salts from municipal solid waste combustion residues. Waste Manag. 23, 291–305. https://doi.org/10.1016/s0956-053x(02)00154-x.

Alba, N., Gassó, S., Lacorte, T., Baldasano, J.M., 1997. Characterization of municipal solid waste incineration residues from facilities with different air pollution control systems. J. Air Waste Manag. Assoc. 47, 1170–1179. https://doi.org/10.1080/10473289.1997.10464059.

Aubert, J.E., Husson, B., Sarramone, N., 2006. Utilization of municipal solid waste incineration (MSWI) fly ash in blended cement Part 1: processing and characterization of MSWI fly ash. J. Hazard Mater. 136, 624–631. https://doi.org/10.1016/j.jhazmat.2005.12.041.

Chimenos, J., Segarra, M., Fernández, M., Espiell, F., 1999. Characterization of the bottom ash in municipal solid waste incinerator. J. Hazard Mater. 64, 211–222. https://doi.org/10.1016/S0304-3894(98)00246-5.

Cornelis, G., Gerven, T.V., Vandecasteele, C., 2012. Antimony leaching from MSWI bottom ash: modelling of the effect of pH and carbonation. Waste Manag. 32, 278–286. https://doi.org/10.1016/j.wasman.2011.09.018.

Dabo, D., Badreddine, R., De Windt, L., Drouadaine, I., 2009. Ten-year chemical evolution of leachate and municipal solid waste incineration bottom ash used in a test road site. J. Hazard Mater. 172, 904–913. https://doi.org/10.1016/j.jhazmat.2009.07.083.

Dabo, D., Raimbault, L., Badreddine, R., Chaurand, P., Rose, J., Windt, L.De, 2008. Characterisation of Glassy and Heterogeneous Cementing Phases of Municipal Solid Waste of Incineration (MSWI) Bottom Ash. AusIMM Publications,

Melbourne, Australia, pp. 95–100.
Dahl, O., Nurmesniemi, H., Pöykiö, R., Watkins, G., 2009. Comparison of the characteristics of bottom ash and fly ash from a medium-size (32 MW) municipal district heating plant incinerating forest residues and peat in a fluidized-bed boiler. Fuel Process. Technol. 90, 871–878. https://doi.org/10.1016/j.fuproc.2009.04.013.
del Valle-Zermeño, R., Gómez-Manrique, J., Giro-Paloma, J., Formosa, J., Chimenos, J.M., 2017. Material characterization of the MSWI bottom ash as a function of particle size. Effects of glass recycling over time. Sci. Total Environ. 581–582, 897–905. https://doi.org/10.1016/j.scitotenv.2017.01.047.
Dijkstra, J.J., Van Der Sloot, H.A., Comans, R.N.J., 2006. The leaching of major and trace elements from MSWI bottom ash as a function of pH and time. Appl. Geochem. 21, 335–351. https://doi.org/10.1016/j.apgeochem.2005.11.003.
Fällman, A.M., Hartlén, J., 1994. Leaching of slags and ashes - controlling factors in field experiments versus in laboratory tests. Environ. Aspects Construct. Waste Mat. 39–54. https://doi.org/10.1016/s0166-1116(08)71446-8.
Gao, X., Yuan, B., Yu, Q.L., Brouwers, H.J.H., 2017. Characterization and application of municipal solid waste incineration (MSWI) bottom ash and waste granite powder in alkali activated slag. J. Clean. Prod. 164, 410–419. https://doi.org/10.1016/j.jclepro.2017.06.218.
Grossman, D.G., 1972. Machinable glass-ceramics based on tetrasilicic mica. J. Am. Ceram. Soc. 55, 446–449. https://doi.org/10.1111/j.1151-2916.1972.tb11337.x.
Hui, K.S., Chao, C.Y.H., 2006. Pure, single phase, high crystalline, chamfered-edge zeolite 4A synthesized from coal fly ash for use as a builder in detergents. J. Hazard Mater. 137, 401–409. https://doi.org/10.1016/j.jhazmat.2006.02.014.
Inkaew, K., Saffarzadeh, A., Shimaoka, T., 2015. Modeling the formation of the quench product in municipal solid waste incineration (MSWI) bottom ash. Waste Manag. https://doi.org/10.1016/j.wasman.2016.03.019.
Ito, R., Dodbiba, G., Fujita, T., Ahn, J.W., 2008. Removal of insoluble chloride from bottom ash for recycling. Waste Manag. 28, 1317–1323. https://doi.org/10.1016/j.wasman.2007.05.015.
Iwata, S., Chiba, K., Haraguchi, H., Fujimori, E., Minamoto, K., 2004. Enrichment of elements in industrial waste incineration bottom ashes obtained from three different types of incinerators, as studied by ICP-AES and ICP-MS. J. Mater. Cycles Waste Manag. 6, 73–79. https://doi.org/10.1007/s10163-003-0106-6.
Keulen, A., van Zomeren, A., Harpe, P., Aarnink, W., Simons, H.A.E., Brouwers, H.J.H., 2015. High performance of treated and washed MSWI bottom ash granulates as natural aggregate replacement within earth-moist concrete. Waste Manag. 49, 83–95. https://doi.org/10.1016/j.wasman.2016.01.010.
Kolev, S.D., McKelvie, I.D., 2008. Advances in Flow Injection Analysis and Related Techniques, Comprehensive Analytical Chemistry. Elsevier, Amsterdam, the Netherlands, p. 808.
Lam, C.H.K., Ip, A.W.M., Barford, J.P., McKay, G., 2010. Use of incineration MSW ash: a review. Sustainability 2, 1943–1968. https://doi.org/10.3390/su2071943.
Li, X.-G., Lv, Y., Ma, B.-G., Chen, Q.-B., Yin, X.-B., Jian, S.-W., 2012. Utilization of municipal solid waste incineration bottom ash in blended cement. J. Clean. Prod. 32, 96–100. https://doi.org/10.1016/j.jclepro.2012.03.038.
Lin, W.Y., Heng, K.S., Sun, X., Wang, J.Y., 2015. Accelerated carbonation of different size fractions of MSW IBA and the effect on leaching. Waste Manag. 41 https://doi.org/10.1016/j.wasman.2015.04.003.
Liu, Y., Li, Y., Li, X., Jiang, Y., 2008. Leaching behavior of heavy metals and PAHs from MSWI bottom ash in a long-term static immersing experiment. Waste Manag. 28, 1126–1136. https://doi.org/10.1016/j.wasman.2007.05.014.
Marchese, F., Genon, G., 2011. Effect of leaching behaviour by quenching of bottom ash from MSW incineration. Waste Manag. Res. 29, 39–47. https://doi.org/10.1177/0734242X10387848.
Matusiewicz, H., 2017. Sample preparation for inorganic trace element analysis. Phys. Sci. Rev. 2 (5), 20178001. https://doi.org/10.1515/psr-2017-8001.
Meima, J.A., Comans, R.N., 1999. The leaching of trace elements from municipal solid waste incinerator bottom ash at different stages of weathering. Appl. Geochem. 14, 159–171. https://doi.org/10.1016/S0883-2927(98)00047-X.
Minane, J.R., Becquart, F., Abriak, N.E., Deboffe, C., 2017. Upgraded mineral sand fraction from MSWI bottom ash: an alternative solution for the substitution of natural aggregates in concrete applications. Procedia Eng 180, 1213–1220. https://doi.org/10.1016/j.proeng.2017.04.282.
Polettini, A., Pomi, R., Fortuna, E., 2009. Chemical activation in view of MSWI bottom ash recycling in cement-based systems. J. Hazard Mater. 162, 1292–1299. https://doi.org/10.1016/j.jhazmat.2008.06.018.
Quina, M.J., Bordado, J.C.M., Quinta-Ferreira, R.M., 2009. The influence of pH on the leaching behaviour of inorganic components from municipal solid waste APC residues. Waste Manag. 29, 2483–2493. https://doi.org/10.1016/j.wasman.2009.05.012.
Saffarzadeh, A., Shimaoka, T., Wei, Y., Gardner, K.H., Musselman, C.N., 2011. Impacts of natural weathering on the transformation/neoformation processes in landfilled MSWI bottom ash: a geoenvironmental perspective. Waste Manag. 31, 2440–2454. https://doi.org/10.1016/j.wasman.2011.07.017.
Saqib, N., Bäckström, M., 2016. Chemical association and mobility of trace elements in 13 different fuel incineration bottom ashes. Fuel 172. https://doi.org/10.1016/j.fuel.2016.01.010.
Schollbach, K., Alam, Q., Caprai, V., Florea, M.V.A., Laan, S.R. van der, Hoek, C.J.G. van, Brouwers, H.J.H., 2016. Combined characterization of MSWI bottom ash. In: Proc. The 38th International Cement Microscopy Association (ICMA) Conference. April 17-21, 2016, Lyon, France URL. research.tue.nl/en/publications/combined-characterization-of-mswi-bottom-ash. (Accessed 23 September 2018).
Sormunen, L.A., Kalliainen, A., Kolisoja, P., Rantsi, R., 2017. Combining mineral fractions of recovered MSWI bottom ash: improvement for utilization in civil engineering structures. Waste and Biomass Valorization 8, 1467–1478. https://doi.org/10.1007/s12649-016-9656-4.
Speiser, C., Baumann, T., Niessner, R., 2001. Characterization of municipal solid waste incineration (MSWI) bottom ash by scanning electron microscopy and quantitative energy dispersive X-ray microanalysis (SEM/EDX). Fresenius' J. Anal. Chem. 370, 752–759. https://doi.org/10.1007/s002160000659.
Sunda, W.G., Lewis, J.A.M., 1978. Effect of complexation by natural organic ligands on the toxicity of copper to a unicellular alga, *Monochrysis lutheri* 1. Limnol. Oceanogr. 23, 870–876. https://doi.org/10.4319/lo.1978.23.5.0870.
Tang, P., Florea, M.V.A., Brouwers, H.J.H., 2017. Employing cold bonded pelletization to produce lightweight aggregates from incineration fine bottom ash. J. Clean. Prod. 165, 1371–1384. https://doi.org/10.1016/J.JCLEPRO.2017.07.234.
Tasneem, K.M., Nam, B.H., Eun, J., 2015. Sustainable utilization of MSWI bottom ash as road construction materials, Part II: chemical and environmental characterization. In: Airfield and Highway Pavements 2015. American Society of Civil Engineers, Reston, VA, pp. 593–604. https://doi.org/10.1061/9780784479216.053.
van der Sloot, H.A., Heasman, L., Quevauviller, P., 1997. Harmonization of leaching/extraction tests. Stud. Environ. Sci. https://doi.org/10.1016/S0166-1116(97)80109-4.
Vasiliev, L.L., Kanonchik, L.E., Antuh, A.A., Kulakov, A.G., 1996. NaX zeolite, carbon fibre and CaCl2 ammonia reactors for heat pumps and refrigerators. Adsorption 2, 311–316. https://doi.org/10.1007/BF00879546.
Verbinnen, B., Van Caneghem, J., Billen, P., Vandecasteele, C., 2017. Long term leaching behavior of antimony from MSWI bottom ash: influence of mineral additives and of organic acids. Waste. Biomass Valorization 8, 2545–2552. https://doi.org/10.1007/s12649-016-9796-6.
Wei, Y., Shimaoka, T., Saffarzadeh, A., Takahashi, F., 2011. Mineralogical characterization of municipal solid waste incineration bottom ash with an emphasis on heavy metal-bearing phases. J. Hazard Mater. 187, 534–543. https://doi.org/10.1016/j.jhazmat.2011.01.070.
Wiles, C.C., 1995. Municipal solid waste combustion ash : state of the knowledge. J. Hazard Mater. 3894, 20. https://doi.org/10.1016/0304-3894(95)00120-4.
Wongsa, A., Boonserm, K., Waisurasingha, C., Sata, V., Chindaprasirt, P., 2017. Use of municipal solid waste incinerator (MSWI) bottom ash in high calcium fly ash geopolymer matrix. J. Clean. Prod. 148, 49–59. https://doi.org/10.1016/j.jclepro.2017.01.147.
Wu, B., Wang, D., Chai, X., Takahashi, F., Shimaoka, T., 2016. Characterization of chlorine and heavy metals for the potential recycling of bottom ash from municipal solid waste incinerators as cement additives. Front. Environ. Sci. Eng. 10, 8. https://doi.org/10.1007/s11783-016-0847-9.
Xing, W., Hendriks, C., 2006. Decontamination of granular wastes by mining separation techniques. J. Clean. Prod. 14, 748–753. https://doi.org/10.1016/J.JCLEPRO.2004.05.007.
Yao, J., Li, W.B., Tang, M., Fang, C.R., Feng, H.J., Shen, D.S., 2010. Effect of weathering treatment on the fractionation and leaching behavior of copper in municipal solid waste incinerator bottom ash. Chemosphere 81, 571–576. https://doi.org/10.1016/j.chemosphere.2010.08.038.
Zevenbergen, C., Wood, T.V., Bradley, J.P., Van der Broeck, P.F.C.W., Orbons, A.J., Van Reeuwijk, L.P., 1994. Morphological and chemical properties of MSWI bottom ash with respect to the glassy constituents. Hazard Waste Hazard. Mater. 11, 371–383. https://doi.org/10.1089/hwm.1994.11.371.
Zhu, W., Chen, X., Struble, L.J., Yang, E.-H., 2018. Characterization of calcium-containing phases in alkali-activated municipal solid waste incineration bottom ash binder through chemical extraction and deconvoluted Fourier transform infrared spectra. J. Clean. Prod. 192, 782–789. https://doi.org/10.1016/j.jclepro.2018.05.049.